HHS Public Access

Author manuscript

Arterioscler Thromb Vasc Biol. Author manuscript; available in PMC 2021 July 01.

Published in final edited form as:

Arterioscler Thromb Vasc Biol. 2020 July ; 40(7): e203–e213. doi:10.1161/ATVBAHA.119.313848.

Transforming growth factor-β–activated kinase 1 regulates arteriovenous fistula maturation

Haidi Hu[1,2,3], **Shin-Rong Lee**[2,3], **Hualong Bai**[2,3], **Jiangming Guo**[2,3], **Takuya Hashimoto**[2,3], **Toshihiko Isaji**[2,3], **Xiangjiang Guo**[2,3], **Tun Wang**[2,3], **Katherine Wolf**[2,3], **Shirley Liu**[2,3], **Shun Ono**[2,3], **Bogdan Yatsula**[2,3], **Alan Dardik**[2,3,4]

[1]Department of Vascular and Thyroid Surgery, the First Hospital of China Medical University, Shenyang, China

[2]Department of Surgery, Yale University School of Medicine, New Haven, CT, USA

[3]Vascular Biology and Therapeutics Program, Yale University School of Medicine, New Haven, CT, USA

[4]VA Connecticut Healthcare Systems, West Haven, CT, USA

Abstract

Objective-----—Arteriovenous fistulae (AVF) are the optimal conduit for hemodialysis access but have high rates of primary maturation failure. Successful AVF maturation requires deposition of extracellular matrix (ECM) including collagen and fibronectin, as well as orderly temporal regulation of ECM components. Transforming growth factor-β–activated kinase 1 (TAK1) is a mediator of non-canonical TGFβ signaling and plays crucial roles in regulation of ECM production and deposition; therefore, we hypothesized that TAK1 regulates wall thickening during AVF maturation by alteration of expression of components of the ECM.

Approach and Results-----—In both human and mouse AVF, immunoreactivity of TAK1, c-Jun N-terminal kinase, p38, collagen-1 and fibronectin were significantly increased compared to control veins. Manipulation of TAK1 *in vivo* altered AVF wall thickening and luminal diameter; reduced TAK1 function was associated with reduced thickness and smaller diameter, whereas activation of TAK1 function was associated with increased thickness and larger diameter. Arterial magnitudes of laminar shear stress (20 dyne/cm^2) activated non-canonical TGFβ signaling including TAK1 phosphorylation in mouse endothelial cells.

Conclusions-----—TAK1 is increased in AVF, and TAK1 manipulation in a mouse AVF model regulates AVF thickness and diameter. Targeting non-canonical TGFβ signaling such as TAK1 might be a novel therapeutic approach to improve AVF maturation.

Graphical Abstract

To whom correspondence should be addressed: Alan Dardik, MD, PhD, Yale University School of Medicine, 10 Amistad Street, Room 437, PO Box 208089, New Haven, CT 06520-8089 USA. Tel: +1 203-737-2082. alan.dardik@yale.edu.

Disclosures

None.

Keywords

Arteriovenous fistulae; Maturation; Transforming growth factor-β–activated kinase 1 (TAK1); Shear stress; Mice

Introduction

The worldwide increase of chronic kidney disease has led to increased prevalence of end stage renal disease (ESRD) requiring life-long replacement of kidney function.[1, 2] A functional high-flow vascular access for hemodialysis is the life-line for most patients with ESRD. Although arteriovenous fistulae (AVF) are the preferred conduit for hemodialysis, with superior patency and fewer complications compared with arteriovenous grafts and catheters,[3–5] AVF are far from optimal with a high rate of primary failure of maturation,[6, 7] with some studies reporting up to 60% of AVF failing to support hemodialysis by 5 months.[6]

AVF maturation requires adaptive vascular remodeling to the dramatic hemodynamic changes that occur immediately after AVF creation. Immediately after creation of the arteriovenous anastomosis, the vein is exposed to a high flow, high shear stress, high pressure, and oxygen-rich arterial environment. Endothelial cells detect and respond to these dramatic hemodynamic changes by triggering cascades of signaling pathways that induce structural and functional changes to the vascular wall that stimulate venous wall thickening and lumen dilation.[8, 9] This dramatic remodeling of the vein is essential in order to sustain the high flows necessary for supporting hemodialysis. Unfortunately, the molecular mechanisms that govern this aspect of venous adaptation remain poorly understood, hindering efforts to rationally design therapeutics that can increase fistula maturation.

Using a murine model of AVF that has previously been shown to recapitulate essential features of human AVF maturation,[10] including an early maturation phase with progressive venous wall thickening and lumen dilation, we determine the role of transforming growth factor-β-activated kinase 1 (TAK1) in early AVF maturation. TAK1, also known as MAP3K7, is a key member of the TGF-β non-canonical signaling pathway that has been implicated as an important contributor to vascular development and injury-induced arterial remodeling.[11–13] TAK1 activates downstream effectors such as p38 and c-Jun N-terminal kinase (JNK) to maintain endothelial cell (EC) homeostasis, induce the production and deposition of fibronectin and collagen, and regulate stress-activated cell signaling and survival .[14–21] Since these are cellular functions that are also important for venous remodeling, we hypothesized that TAK1 regulates wall thickening and outward remodeling during AVF maturation.

Materials and Methods

Data Disclosure

The data that support the findings of this study are available from the corresponding author upon reasonable request.

Reagents and antibodies

5Z-7-oxozeaenol (OZ) (Millipore Sigma, 49610), which is an irreversible active site inhibitor of TAK1; TAK1 shRNA lentiviral particles (sc-36607-V, Santa Cruz, CA, USA), which contains 3–5 expression constructs each encoding target-specific shRNA designed to knockdown TAK1 gene expression; Control shRNA lentiviral Particles-A (sc-108080, Santa Cruz, CA, USA), containing scrambled shRNA; CopGFP control lentiviral particles (sc-108084, Santa Cruz, CA, USA); TAK1 lentiviral activation particles (m2) (sc-424044-LAC-2, Santa Cruz, CA, USA), which is a CRISPR-based transcription activation construct packaged into a single lentivirus that upregulates endogenous TAK1; Polybrene® (sc-134220, Santa Cruz, CA, USA); Puromycin dihydrochloride (sc-108071, Santa Cruz, CA, USA).

Primary antibodies included: anti-α-actin (Abcam, ab5694; IHC and IF, 5μg/ml); anti-vWF (Abcam, ab11713; IF, 10μg/ml); anti-cleaved caspase-3 (Cell Signaling #9661; IHC, 1μg/ml); anti-collagen I (Abcam, ab34710; IF, 5μg/ml); anti-fibronectin (Abcam, ab2413; IF, 25μg/ml); anti-GAPDH (Cell Signaling #2118; WB, 0.021μg/ml); anti-proliferating cell nuclear antigen (PCNA) (Dako, #M0879; IF, 5μg/ml); phospho-TAK1 (Abcam, ab109404; WB, 0.018μg/ml); anti-TAK (ThermoFisher, PA5–20083; IF, 20μg/ml; WB, 2μg/ml); control rabbit IgG (Santa Cruz, sc-2027, 1–20 μg/ml). Antibodies were verified with Western blots showing a band at the anticipated molecular weight of the protein.

Secondary antibodies used for immunofluorescence (IF) were: donkey anti-goat Alexa-Fluor-488, donkey anti-rabbit Alexa-Fluor-488, donkey anti-rabbit Alexa-Fluor-568, donkey antimouse Alexa-Fluor-568 and chicken anti-mouse Alexa-Fluor-488 conjugated antibodies from Invitrogen (2μg/ml). For IHC, sections were incubated with EnVision reagents for 1 h at room temperature and treated with Dako Liquid DAB+ Substrate Chromogen System (Dako). Finally, the sections were counterstained with Mayer’s hematoxylin.

Human AVF sample collection

This study was approved by the Human Investigation Committee of VA Connecticut and patients gave informed consent to use the samples. Deidentified vein and AVF samples were collected from patients with ESRD undergoing AVF creation or revision. Control veins and AVF were unmatched samples from different patients. The control veins were veins that did not have an AVF but were discarded as part of the operative procedure. The AVF were small mature AVF segments that were harvested during surgical revision procedures for focal stenoses but did not include the actual lesion itself. All the AVF were mature segments previously used for hemodialysis that were harvested at least 6 months after the original AVF creation procedure. Part of the samples were formalin fixed and paraffin embedded, and another part was frozen at −80°C.

Animal Model

Ten-week-old male C57BL/6J mice (The Jackson Laboratory; Bar Harbor, ME) were used and maintained as previously described.[22] Only male mice were used because of sex-specific differences in AVF maturation, as previously reported in multiple clinical studies.[23–25] All animal experiments were performed in accordance with federal guidelines and Yale University Institutional Animal Care and Use Committee approval. Anesthesia was administered using 2–3% isoflurane, and post-operative pain control was provided for 48 hours after surgery with 0.1mg/kg buprenorphine delivered intraperitoneally. AVF were created with a 25-gauge needle puncturing through the aorta into the IVC, as shown in figure I in the supplement, and as previously reported.[10, 26] Successful creation of an AVF was confirmed by direct visualization of pulsatile arterial blood flow in the IVC, as well as elevated aortic diastolic flow on serial Doppler ultrasound. The venous limb of the AVF was harvested at baseline, or on post-operative days 7, 14 or 21. Only successfully matured AVF were used in this study; thrombosed AVF due to technical failure were excluded.

For chemical inhibition of TAK1, either OZ (10% DMSO in saline) or vehicle was administered at 0.5mg/kg daily for 7 days from the day of AVF creation to post-operative day 7. For lentiviral experiments (including lentiviral control particles, lentiviral TAK1 shRNA or lentiviral TAK1 activation particles), 20 μL (1×10^8 pfu/mL) of control, shRNA or activation particle lentivirus was mixed with 100 μL of 25% pluronic F-127 gel (Invitrogen, USA) and 0.2 μL Polybrene® (sc-134220) and applied periadventitially on the infrarenal IVC during the time of sham/AVF creation and incubated for 5 minutes prior to abdominal closure.

Doppler ultrasound (Vevo 770 High-Resolution Imaging System (Fujifilm VisualSonics; Toronto, Canada) with probe RMV70, 20–60 MHz) was performed at baseline and post-operatively on days 7, 14 and 21 to confirm AVF patency and to measure the diameter of the aorta and IVC immediately inferior to the left renal vein (see figure I in the supplement), as previous reported.[10]

Cell culture

Mouse lung endothelial cells (EC) were prepared and cultured as previously described.[27, 28] The sex of EC used was not determined. Briefly, EC were cultured in endothelial basal medium 2 (EBM-2) with endothelial cell growth media-2 MV SingleQuot Kit Supplement & Growth Factors (Lonza), 20% FBS (Gibco) and 1% penicillin/streptomycin (Gibco), 2 mM L-glutamine (Corning Life Sciences).

In vitro TAK1 manipulation

EC at 50% confluence in 6 well plates were transduced with lentivirus (20 μL of 1×10^8 pfu/mL control, TAK1 shRNA or TAK1 activation particles with 0.2 μL Polybrene® (sc-134220) in Opti-MEM (ThermoFisher Scientific, MA)) after serum starvation for 6 hours. After incubation for 6 hours, media was exchanged for full endothelial basal medium containing growth factors, 20% FBS and antibiotics as described above. After 24 hrs, the EC were replaced with fresh medium containing puromycin (2.0μg/ml; Santa Cruz, CA). After puromycin selection for 1 week, the cells were used for shear stress experiments.

Laminar shear stress experiment

EC were seeded and cultured on collagen I-coated glass plates (StreamerTM Culture Slips, Flexcell Corporation) until approximately 80% confluent and then serum-starved for 24 hrs. In some experiments the EC were pre-treated with OZ (1 μM) or vehicle for 1 hr in incubator (37 °C, 5% CO2).. EC were exposed to laminar shear stress using a parallel-plate flow chamber with circulating EBM-2 medium (0% FBS, 37 ± 0.5 °C), as previously described.[27] The magnitude of shear stress was set at 0 dynes/cm^2, 3 dynes/cm^2 or 20 dynes/cm^2. After 1 hour of shear stress treatment, slides were washed twice with cold PBS, EC were removed with RIPA lysis buffer and cell lysate extracted for further study.

Western Blot

Total protein in tissues or EC was extracted using RIPA Lysis Buffer (Beyotime); protein concentrations were assessed using a colorimetric assay (Bio-Rad; Hercules, CA). For immunoblotting, proteins (20–40 μg) were separated on a 8–10% SDS-PAGE gel and electrophoretically transferred to a polyvinylidene difluoride microporous membrane (0.45 μm pore size, Immobilon, Millipore), and blocked in TBS-T containing 5% bovine serum albumin for 1 h at room temperature, then blotted with primary antibody of targeted proteins overnight at 4 °C on a shaker. After washing the membranes with TBS-T and incubating them with either anti-rabbit or anti-mouse horseradish peroxidase-conjugated secondary antibody for 1 h at room temperature, the membranes were developed using the Western Lightning Plus ECL reagent (PerkinElmer; Waltham, MA). Where needed, membranes were stripped with Restore Western Blot Stripping Buffer (Pierce Biotechnology; Rockford, IL) and re-probed as described above.

RNA Extraction and Real-Time Quantitative Polymerase Chain Reaction

Total RNA was isolated from tissue by using RNeasy Mini Kit with digested DNase I (Qiagen; Valencia, CA). RNA quality was confirmed using a NanoDrop spectrophotometer at the 260/280nm ratio (Thermo Scientific; Wilmington, DE). Reverse transcription was performed using SuperScript III First-Strand Synthesis Supermix (Invitrogen). Real-time PCR was performed using iQ SYBR Green Supermix (Bio-Rad) and amplified for 40 cycles using the iQ5 Real-Time PCR Detection System (Bio-Rad). Correct target amplification and exclusion of nonspecific amplification was confirmed by 1.5% agarose gel electrophoresis and melt curve analysis. Primers of mouse TAK1 are as following: forward primer: GTGGGGGACGAGTACGAGAT, reverse primer: TGGTCACCACATCAAAAGCAT. Primers for mouse β-actin: forward primer: GGCTGTATTCCCCTCCATCG, reverse primer: CCAGTTGGTAACAATGCCATGT. All samples were normalized to β-actin amplification and graphed in relative units.

Histology

Mouse AVF samples were obtained after flushing with cold PBS followed by 10% neutralized buffered formalin. The tissue block was then embedded in paraffin, cut in 5 μm cross-sections, with 3–5 consecutive sections mounted onto each glass slide. Sections were obtained from 50 through 150 um cranial to the arteriovenous anastomosis where the remodeled vein is more uniform. IVC sections from sham experiments were obtained

approximately 5 mm cranial to the aortic bifurcation. Hematoxylin and eosin (H&E), Masson's trichrome, and Elastin Von Gieson (EVG) staining were used to observe morphology. Wall (intima-media) thickness was measured in one section per sample using ImageJ software (National Institutes of Health; Bethesda, MD) by taking the average of thickness measured at 8 points around the vessel circumference, as previously described.[10, 29]

Immunofluorescence

Tissue sections were de-paraffined using xylene and a graded series of alcohols. For antigen-retrieval, sections were heated in citric acid buffer (pH 6.0) at 100°C for 10 minutes. After washing, sections were blocked with 5% normal goat serum in PBS (pH 7.4) for 1 hr at room temperature to block non-specific protein binding sites. Sections were then incubated at 4°C with the primary antibody. Negative controls included incubation in blocking buffer without primary antibody, or with isotype control immunoglobulin, and were performed with each experiment to rule out false positive results. After overnight incubation, sections were incubated with second antibodies for 1hr at room temperature. Secondary antibodies were: donkey anti-rabbit Alexa-Fluor-488 and donkey anti-rabbit Alexa-Fluor-568 conjugated antibodies (Invitrogen; Carlsbad, CA). Sections were stained with 4',6-diamidino-2-phenylindole (DAPI) (Invitrogen) to stain cellular nuclei. Positively staining cells were counted in the presence of well-defined nuclei per high power field. The integrated density of matrix (collagen I and Fibronectin) expression in the vessel wall was analyzed using ImageJ software (National Institutes of Health; Bethesda, MD), and reflects the total fluorescence within the region-of-interest.

Statistical Analysis

Data was collected and measured by a single, non-blinded observer. Data are represented as mean ± SEM. All data was analyzed using Prism 7 software (GraphPad Software; La Jolla, CA). Data were assumed to be from a normal distribution with equal variance, as suggested by normality (D'Agostino & Pearson test or Shapiro-Wilk test) and F tests. Statistical significance for these analyses was determined using Student's t-test, or ANOVA (with repeated measures for time-series data) with the Sidak post hoc correction. P values of less than 0.05 were considered statistically significant.

Results

1. TAK1 expression is increased in human AVF

Since TAK1 regulates production and deposition of collagen I and fibronectin [11, 12, 14–16, 30], we hypothesized that TAK1 would be expressed in successfully matured AVF. Mature AVF and veins from patients undergoing surgical revision were analyzed. AVF exhibited significantly increased wall (intima-media) thickness and outward remodeling (lumen dilation) compared to control veins (Figure 1A), as required to accommodate the increased blood flow to achieve successful hemodialysis. There was increased immunoreactivity of total and phosphorylated TAK1, and its downstream signaling effectors JNK and p38[17, 19, 31] in the mature AVF compared to the control vein (Figure 1B), without change in phospho:total TAK1 (Figure IIA in the supplement). In addition, there was also increased

expression of Akt1 and ERK1/2 (Figure IIA in the supplement). Increased TAK1 expression was present both in endothelial cells (EC) as well as in smooth muscle cells (SMC) (Figure 1C). There was also increased collagen deposition in mature human AVF in all 3 layers of vessel wall on trichrome stain (Figure IIB in the supplement). Using immunofluorescence, total collagen I immunoreactivity was increased in both the intima and media of mature AVF compared to control veins (Figure 1D). Similarly, total fibronectin immunoreactivity was also increased in AVF compared to control, but the increase in the medial layer did not reach statistical significance (Figure 1E). These results show that increased immunoreactivity of TAK1 and its downstream effectors correlate with increased total collagen and fibronectin deposition in mature human AVF.

2. TAK1 expression is increased in mouse AVF

We next determined whether TAK1 was also expressed in mouse AVF. TAK1 mRNA expression was significantly increased in the mouse AVF (day 21) compared to both baseline IVC (day 0) and sham IVC (day 21) (Figure IIIA in the supplement). Immunoreactivity of phospho and total TAK1, JNK, and p38 as well as Akt1 and ERK1/2 were significantly increased in mouse AVF compared to sham at day 21, without change in phospho:total TAK1 (Figure 2A, Figure IIIB in the supplement). Increased TAK1 immunoreactivity was observed in both EC and in SMC (Figure 2B), and both total collagen I and fibronectin immunoreactivity were also increased in mouse AVF compared to sham (day 21; Figure 2C–D). These results are similar to those in human patients (Figure 1) and suggest that TAK1 might be a mechanism that regulates AVF maturation.

3. TAK1 manipulation mediates AVF wall thickening and diameter *in vivo*

We next determined whether TAK1 mediates AVF maturation by manipulating TAK1 activity *in vivo*. We treated mice with 5Z-7-oxozeaenol (OZ), a chemical compound that irreversibly binds to the ATP binding sites of TAK1, thereby selectively inhibiting TAK1 kinase activity,[32, 33] or control vehicle for 7 days from the day of surgery. Mice treated with OZ showed decreased AVF wall (intima-media) thickness compared with control AVF treated with vehicle alone at 21 days post-op (Figure 3A). There was also less AVF dilation in mice treated with OZ compared to control mice (Figure 3B) while the aortic diameter remained unchanged (Figure IVA in the supplement). The reduced AVF wall thickness in mice treated with OZ was characterized by reduced proliferation (Figure 3C) without increased apoptosis (Figure 3D). In addition, there was reduced total collagen I (Figure 3E) and reduced total fibronectin (Figure 3F) immunoreactivity within the vessel wall of mice treated with OZ compared to vehicle. OZ treatment did not affect macrophage infiltration into the venous wall (day 21; Figure VA in the supplement).

We next reduced TAK1 signaling by treating AVF with lentivirally delivered TAK1-specific shRNA applied periadventitially in pluronic gel during the time of surgery. We first confirmed *in vitro* that TAK1-specific shRNA reduced TAK1 protein expression in EC (Figure VI in the supplement). Because our lentiviral constructs were not fluorescently-tagged, we used periadventitial application of GFP lentiviral particles to confirm that lentivirus delivered transgenes into the whole vessel wall, including the intima (Figure VII in the supplement), consistent with prior reports.[27, 34]

Treatment with TAK1-specific shRNA *in vivo* resulted in significantly reduced wall thickening (Figure 3G) and AVF diameter (Figure 3H) compared to controls, without any significant effect on aortic diameter (Figure IVB in the supplement). Treatment with TAK1-specific shRNA was also associated with reduced proliferation (Figure 3I) without any increase in apoptosis (Figure 3J), as well as reduced total collagen 1 (Figure 3K) and total fibronectin (Figure 3L) immunoreactivity within the vessel wall. Macrophage infiltration was unaffected by TAK1-specific shRNA treatment (Figure VB in supplement).

We next determined the effects of increased TAK1 expression, using TAK1 lentiviral activation particles to overexpress TAK1 (Figure VIB in the supplement). Overexpression of TAK1 using lentiviral activation particles by periadventitial transduction *in vivo* was associated with increased wall thickening (Figure 3M) as well as increased AVF diameter (Figure 3N), without significant change in aortic diameter (Figure IVC in the supplement), compared to control lentivirus. TAK1 overexpression was also associated with increased proliferation (Figure 3O) without decreased apoptosis (Figure 3P), as well as increased total collagen 1 (Figure 3Q) and fibronectin (Figure 3R) immunoreactivity in the vessel wall. Macrophage infiltration was unaffected by TAK1 overexpression (Figure VC in supplement).

This data shows that reducing or increasing TAK1 signaling results in opposing changes in wall thickness, suggesting that TAK1 signaling mediates wall thickening during AVF maturation.

5. Increased shear stress mediates TAK1 phosphorylation in EC *in vitro*

We next determined whether increased shear stress could be a mechanism for increased TAK1 signaling within endothelial cells, since increased shear stress is an important stimulus of vascular wall remodeling that characterizes AVF maturation.[35–38] We treated mouse endothelial cells (EC) with venous or arterial magnitudes of shear stress *in vitro* and examined TAK1 signaling (Figure 4).

EC showed a low amount of TAK1 phosphorylation under both static conditions as well as with venous (3 dyne/cm^2) magnitudes of shear stress (Figure 4A,C,D). In contrast, arterial (20 dyne/cm^2) magnitudes of shear increased TAK1 phosphorylation by 3-fold (Figure 4C,D). Interestingly, the arterial shear-stress mediated increase in TAK1 phosphorylation was blocked with administration of the TAK1-specific inhibitor OZ (Figure 4C,D), but without affecting total TAK1 levels (Figure 4B); this is consistent with other in vitro studies that show OZ-mediated reduction in phospho-TAK1 immunoreactivity,[39, 40] and might reflect inhibition of TAK1 autophosphorylation by OZ.[32] Signaling molecules downstream of TAK1 such as JNK and p38 were similarly activated with increased phospho-to-total ratios (6-fold, and 4.5-fold respectively) under arterial shear stress, which were reduced to baseline levels with OZ (Figure 4E,F). Administration of TAK1-specific shRNA knocked down total TAK1 as well as phospho-TAK1 levels (Figure 4G–I) without affecting phospho:total TAK1 (Figure 4J). The decrease in both total and phospho-TAK1 levels was associated with decreased shear-stress-stimulated phospho:total JNK, and p38 immunoreactivity (Figure 4K,L). On the other hand, increasing total TAK1 via use of lentiviral TAK1 activation particles (Figure 4M–O) similarly led to accentuation of shear-

stress mediated increases in phospho:total TAK1, JNK and p38 (Figure 4P–R). Arterial magnitudes of shear stress also increased eNOS, Akt1 and ERK1/2 phosphorylation, and this was inhibited either by OZ or TAK1-specific shRNA, and increased further with TAK1 activation particles (Figure VIII in the supplement).

This data is consistent with arterial magnitudes of shear stress increasing TAK1 phosphorylation as well as phosphorylation of its downstream effectors in EC; inhibition of TAK1 blunts these responses while TAK1 overexpression augments these responses. These results suggest that TAK1 activation in endothelial cells regulate shear stress-induced signaling and thus may be an important mechanism of AVF maturation.

Discussion

This paper establishes a role for TAK1 signaling in AVF maturation. We show that TAK1 immunoreactivity is increased in mature human and mouse AVF, and is associated both with increased wall thickening, and increased outward remodeling. TAK1 signaling is increased by arterial magnitudes of shear stress in endothelial cells *in vitro*, suggesting that AVF-induced hemodynamic alterations are an important mechanism of increased TAK1 signaling within the endothelium *in vivo*. Therefore, this data suggests a novel and critical role of TAK1 signaling during AVF maturation.

TAK1 signaling plays a critical role in diverse aspects of physiology and pathology from regulating immune function[41, 42] and cardiovascular development and hypertrophy[12, 43–47] to mediating tumor proliferation[48, 49] and development of chemoresistance.[50] This might be due in part to TAK1's important roles in regulating cell survival, proliferation, and fibrosis.[14–16][51, 52] Therefore, our data showing that TAK1 is important for AVF maturation, a process that requires cellular proliferation and ECM deposition, is consistent with TAK1's known functions.

Although TAK1 immunoreactivity was increased in both EC and SMC in the AVF, the TAK1-triggered signal transduction pathways and endpoints are likely different for the two cell types. For example, the data showing the effects of TAK1 inhibition or activation with proliferation and ECM deposition (Figure 3) likely represent an SMC-specific response to TAK1 manipulation, as most PCNA positive cells were SM-actin positive, and medial ECM synthesis and deposition are largely secreted by SMC.[53] Consistent with prior studies showing that TAK1 activity is required for growth-factor induced proliferation of airway smooth muscle cells[54] and TAK1's role in ECM deposition,[14–16] our data suggests that TAK1 signaling also mediates AVF-induced SMC proliferation and might regulate collagen 1 and fibronectin expression. The role of increased TAK1 signaling within EC during AVF maturation is less clear, but recent studies showing that TAK1 inhibits inflammation-induced EC cell death[55, 56] suggest that increased TAK1 in EC might serve a protective mechanism within the inflammatory environment of AVF maturation. It is important to note that while we can conclude from our experiments that altering TAK1 within the vascular wall mediates wall thickening, we were unable to determine in our mechanistic studies the relative contributions of TAK1 signaling within each cell type to AVF maturation. This is because our lentiviral constructs were driven by universal promoters, and the transduction efficiency

of each construct within each cell type could not be easily determined as the constructs were not tagged. Given the distinct physiologic roles of EC and SMC in AVF maturation, determining the impact of cell-specific TAK1 manipulation on venous remodeling will be an interesting point of future study.

Our *in vitro* shear stress data shows that arterial magnitudes of shear stress activates TAK1 (Figure 4), suggesting one possible mechanism of increased TAK1 signaling in endothelial cells *in vivo*. However, this finding differs from a prior study that showed TAK1 signaling was decreased with arterial shear stress.[57] This discrepancy could be due to several factors: whereas we investigated TAK1 activity under acute (1 hour), serum-starved conditions in mouse lung endothelial cells, Lee et al.[57] performed their investigations under chronic (48 hours), stressed (oxidative stress + TGFβ1 stimulation) and growth factor rich (20% fetal bovine serum) conditions in human umbilical vein endothelial cells. Our results are consistent with other reports that shear stress induces TGFβ secretion *in vitro*;[58–60] this increased TGFβ would be expected to subsequently stimulate downstream TGFβ signaling, resulting in increased TAK1 signaling as seen in Figure 4. Although it is not clear which *in vitro* experimental model best recapitulates the *in vivo* endothelial environment during AVF creation and maturation, our model has the advantage that it is consistent with the increased TAK1 seen *in vivo* in mouse and human AVF (Figures 1 and 2). The mechanism by which TAK1 signaling is increased in SMC remains unclear, but it is possible that shear-stress mediated release of TGFβ by EC also stimulates SMC TGFβ signaling in a paracrine fashion. Since shear stress also induces release of other SMC mitogens and chemoattractants (PDGF-BB and IL-1 alpha) from EC *in vitro*,[38] it is possible that shear stress-mediated EC signaling may trigger and regulate vascular remodeling during AVF maturation in vivo.[8, 9]

Lastly, our endothelial cell experiments also suggest JNK and p38 as downstream effectors of shear-stress induced TAK1 activation (Figure 4). These data show that the activation states of JNK and p38, represented by their respective phospho:total levels, are proportional to the amount of phosphorylated TAK1 (pTAK1/GAPDH), since the lentiviral manipulations alter total TAK1 levels without influencing its shear-stress dependent activation (phospho:total TAK1). These results are subtly different from the *in vivo* data (Figure 1B and 2A), which suggest that increased phosphorylated TAK1, JNK and p38 in the AVF were driven by mass effect via increased total TAK1, JNK and p38 levels. However, it is important to note that our Western blots *in vivo* have limited sensitivity for detection of endothelial cell-specific signaling since those assays were performed on proteins isolated from whole vessel walls, of which endothelial cells are a minority cell population. Thus, whether there is also increased phospho:total TAK1, JNK and p38 in endothelial cells *in vivo* in the AVF wall, as suggested by the *in vitro* studies, will be an important point of future work.

In summary, TAK1 regulates AVF maturation in a mouse model. This data suggests that manipulation of the non-canonical TGFβ signaling pathway such as TAK1 may be a novel approach to improving clinical AVF maturation.

Supplementary Material

Refer to Web version on PubMed Central for supplementary material.

Acknowledgments

Sources of Funding

This work was supported the National Institutes of Health Grants R01-HL-128406 and R01-HL-144476, the United States Department of Veterans Affairs Biomedical Laboratory Research and Development Program Merit Review Award I01-BX002336, as well as through the resources and use of facilities at the Veterans Affairs Connecticut Healthcare System (West Haven, CT).

Nonstandard Abbreviations and Acronyms

AVF	arteriovenous fistulae
ECM	extracellular matrix
TGF-β	transforming growth factor-β
TAK1	transforming growth factor-β–activated kinase 1
ESRD	end stage renal disease
CKD	chronic kidney disease
HD	hemodialysis
EC	endothelial cell
SMC	smooth muscle cells
JNK	c-Jun N-terminal kinase
DAPI	4’,6-diamidino-2-phenylindole
OZ	5Z-7-oxozeaenol
eNOS	endothelial nitric oxide synthase

References

1. Jha V, Garcia-Garcia G, Iseki K, Li Z, Naicker S, Plattner B, Saran R, Wang AY, Yang CW. Chronic kidney disease: Global dimension and perspectives. Lancet (London, England). 2013;382:260–272
2. Global, regional, and national age-sex specific all-cause and cause-specific mortality for 240 causes of death, 1990–2013: A systematic analysis for the global burden of disease study 2013. Lancet (London, England). 2015;385:117–171
3. Ravani P, Palmer SC, Oliver MJ, Quinn RR, MacRae JM, Tai DJ, Pannu NI, Thomas C, Hemmelgarn BR, Craig JC, Manns B, Tonelli M, Strippoli GF, James MT. Associations between hemodialysis access type and clinical outcomes: A systematic review. Journal of the American Society of Nephrology : JASN. 2013;24:465–473 [PubMed: 23431075]
4. Santoro D, Benedetto F, Mondello P, Pipito N, Barilla D, Spinelli F, Ricciardi CA, Cernaro V, Buemi M. Vascular access for hemodialysis: Current perspectives. International journal of nephrology and renovascular disease. 2014;7:281–294 [PubMed: 25045278]

5. Almasri J, Alsawas M, Mainou M, Mustafa RA, Wang Z, Woo K, Cull DL, Murad MH. Outcomes of vascular access for hemodialysis: A systematic review and meta-analysis. Journal of vascular surgery. 2016;64:236–243 [PubMed: 27345510]
6. Dember LM, Beck GJ, Allon M, Delmez JA, Dixon BS, Greenberg A, Himmelfarb J, Vazquez MA, Gassman JJ, Greene T, Radeva MK, Braden GL, Ikizler TA, Rocco MV, Davidson IJ, Kaufman JS, Meyers CM, Kusek JW, Feldman HI, Dialysis Access Consortium Study G. Effect of clopidogrel on early failure of arteriovenous fistulas for hemodialysis: A randomized controlled trial. Jama. 2008;299:2164–2171 [PubMed: 18477783]
7. Wilmink T, Hollingworth L, Powers S, Allen C, Dasgupta I. Natural history of common autologous arteriovenous fistulae: Consequences for planning of dialysis. European journal of vascular and endovascular surgery : the official journal of the European Society for Vascular Surgery. 2016;51:134–140
8. Hu H, Patel S, Hanisch JJ, Santana JM, Hashimoto T, Bai H, Kudze T, Foster TR, Guo J, Yatsula B, Tsui J, Dardik A. Future research directions to improve fistula maturation and reduce access failure. Seminars in vascular surgery. 2016;29:153–171 [PubMed: 28779782]
9. Rothuizen TC, Wong C, Quax PH, van Zonneveld AJ, Rabelink TJ, Rotmans JI. Arteriovenous access failure: More than just intimal hyperplasia? Nephrol Dial Transplant. 2013;28:1085–1092 [PubMed: 23543595]
10. Yamamoto K, Protack CD, Tsuneki M, Hall MR, Wong DJ, Lu DY, Assi R, Williams WT, Sadaghianloo N, Bai H, Miyata T, Madri JA, Dardik A. The mouse aortocaval fistula recapitulates human arteriovenous fistula maturation. American journal of physiology. Heart and circulatory physiology. 2013;305:H1718–1725 [PubMed: 24097429]
11. Jadrich JL, O'Connor MB, Coucouvanis E. The tgf beta activated kinase tak1 regulates vascular development in vivo. Development. 2006;133:1529–1541 [PubMed: 16556914]
12. Morioka S, Inagaki M, Komatsu Y, Mishina Y, Matsumoto K, Ninomiya-Tsuji J. Tak1 kinase signaling regulates embryonic angiogenesis by modulating endothelial cell survival and migration. Blood. 2012;120:3846–3857 [PubMed: 22972987]
13. Song Z, Zhu X, Jin R, Wang C, Yan J, Zheng Q, Nanda A, Granger DN, Li G. Roles of the kinase tak1 in cd40-mediated effects on vascular oxidative stress and neointima formation after vascular injury. PloS one. 2014;9:e101671
14. Hocevar BA, Prunier C, Howe PH. Disabled-2 (dab2) mediates transforming growth factor beta (tgfbeta)-stimulated fibronectin synthesis through tgfbeta-activated kinase 1 and activation of the jnk pathway. J Biol Chem. 2005;280:25920–25927 [PubMed: 15894542]
15. Ono K, Ohtomo T, Ninomiya-Tsuji J, Tsuchiya M. A dominant negative tak1 inhibits cellular fibrotic responses induced by tgf-β. Biochemical and Biophysical Research Communications. 2003;307:332–337 [PubMed: 12859960]
16. Kim SI, Kwak JH, Zachariah M, He Y, Wang L, Choi ME. Tgf-beta-activated kinase 1 and tak1-binding protein 1 cooperate to mediate tgf-beta1-induced mkk3-p38 mapk activation and stimulation of type i collagen. Am J Physiol Renal Physiol. 2007;292:F1471–1478 [PubMed: 17299140]
17. Kadohama T, Akasaka N, Nishimura K, Hoshino Y, Sasajima T, Sumpio BE. P38 mitogen-activated protein kinase activation in endothelial cell is implicated in cell alignment and elongation induced by fluid shear stress. Endothelium. 2006;13:43–50 [PubMed: 16885066]
18. Miyagi M, Miwa Y, Takahashi-Yanaga F, Morimoto S, Sasaguri T. Activator protein-1 mediates shear stress-induced prostaglandin d synthase gene expression in vascular endothelial cells. Arterioscler Thromb Vasc Biol. 2005;25:970–975 [PubMed: 15718494]
19. Mengistu M, Brotzman H, Ghadiali S, Lowe-Krentz L. Fluid shear stress-induced jnk activity leads to actin remodeling for cell alignment. J Cell Physiol. 2011;226:110–121 [PubMed: 20626006]
20. Shepherd RD, Kos SM, Rinker KD. Long term shear stress leads to increased phosphorylation of multiple mapk species in cultured human aortic endothelial cells. Biorheology. 2009;46:529–538 [PubMed: 20164634]
21. Yamashita M, Fatyol K, Jin C, Wang X, Liu Z, Zhang YE. Traf6 mediates smad-independent activation of jnk and p38 by tgf-beta. Mol Cell. 2008;31:918–924 [PubMed: 18922473]

22. Tsuneki M, Madri JA. Cd44 regulation of endothelial cell proliferation and apoptosis via modulation of cd31 and ve-cadherin expression. J Biol Chem. 2014;289:5357–5370 [PubMed: 24425872]
23. Masengu A, Maxwell AP, Hanko JB. Investigating clinical predictors of arteriovenous fistula functional patency in a european cohort. Clinical kidney journal. 2016;9:142–147 [PubMed: 26798475]
24. Miller CD, Robbin ML, Allon M. Gender differences in outcomes of arteriovenous fistulas in hemodialysis patients. Kidney international. 2003;63:346–352 [PubMed: 12472802]
25. Miller PE, Tolwani A, Luscy CP, Deierhoi MH, Bailey R, Redden DT, Allon M. Predictors of adequacy of arteriovenous fistulas in hemodialysis patients. Kidney international. 1999;56:275–280 [PubMed: 10411703]
26. Yamamoto K, Li X, Shu C, Miyata T, Dardik A. Technical aspects of the mouse aortocaval fistula. Journal of visualized experiments : JoVE. 2013:e50449
27. Protack CD, Foster TR, Hashimoto T, Yamamoto K, Lee MY, Kraehling JR, Bai H, Hu H, Isaji T, Santana JM, Wang M, Sessa WC, Dardik A. Eph-b4 regulates adaptive venous remodeling to improve arteriovenous fistula patency. Scientific reports. 2017;7:15386 [PubMed: 29133876]
28. Lee MY, Luciano AK, Ackah E, Rodriguez-Vita J, Bancroft TA, Eichmann A, Simons M, Kyriakides TR, Morales-Ruiz M, Sessa WC. Endothelial akt1 mediates angiogenesis by phosphorylating multiple angiogenic substrates. Proc Natl Acad Sci U S A. 2014;111:12865–12870 [PubMed: 25136137]
29. Kuwahara G, Hashimoto T, Tsuneki M, Yamamoto K, Assi R, Foster TR, Hanisch JJ, Bai H, Hu H, Protack CD, Hall MR, Schardt JS, Jay SM, Madri JA, Kodama S, Dardik A. Cd44 promotes inflammation and extracellular matrix production during arteriovenous fistula maturation. Arterioscler Thromb Vasc Biol. 2017;37:1147–1156 [PubMed: 28450292]
30. Li L, Chen Y, Doan J, Murray J, Molkentin JD, Liu Q. Transforming growth factor beta-activated kinase 1 signaling pathway critically regulates myocardial survival and remodeling. Circulation. 2014;130:2162–2172 [PubMed: 25278099]
31. Mu Y, Gudey SK, Landstrom M. Non-smad signaling pathways. Cell Tissue Res. 2012;347:11–20 [PubMed: 21701805]
32. Ninomiya-Tsuji J, Kajino T, Ono K, Ohtomo T, Matsumoto M, Shiina M, Mihara M, Tsuchiya M, Matsumoto K. A resorcylic acid lactone, 5z-7-oxozeaenol, prevents inflammation by inhibiting the catalytic activity of tak1 mapk kinase kinase. J Biol Chem. 2003;278:18485–18490 [PubMed: 12624112]
33. Wu J, Powell F, Larsen NA, Lai Z, Byth KF, Read J, Gu RF, Roth M, Toader D, Saeh JC, Chen H. Mechanism and in vitro pharmacology of tak1 inhibition by (5z)-7-oxozeaenol. ACS Chem Biol. 2013;8:643–650 [PubMed: 23272696]
34. Yang B, Janardhanan R, Vohra P, Greene EL, Bhattacharya S, Withers S, Roy B, Nieves Torres EC, Mandrekar J, Leof EB, Mukhopadhyay D, Misra S. Adventitial transduction of lentivirus-shrna-vegf-a in arteriovenous fistula reduces venous stenosis formation. Kidney international. 2014;85:289–306 [PubMed: 23924957]
35. Chatterjee S Endothelial mechanotransduction, redox signaling and the regulation of vascular inflammatory pathways. Front Physiol. 2018;9:524 [PubMed: 29930512]
36. Remuzzi A, Bozzetto M. Biological and physical factors involved in the maturation of arteriovenous fistula for hemodialysis. Cardiovasc Eng Technol. 2017;8:273–279 [PubMed: 28752375]
37. Caroli A, Manini S, Antiga L, Passera K, Ene-Iordache B, Rota S, Remuzzi G, Bode A, Leermakers J, van de Vosse FN, Vanholder R, Malovrh M, Tordoir J, Remuzzi A, Consortium Ap. Validation of a patient-specific hemodynamic computational model for surgical planning of vascular access in hemodialysis patients. Kidney international. 2013;84:1237–1245 [PubMed: 23715122]
38. Dardik A, Yamashita A, Aziz F, Asada H, Sumpio BE. Shear stress-stimulated endothelial cells induce smooth muscle cell chemotaxis via platelet-derived growth factor-bb and interleukin-1alpha. Journal of vascular surgery. 2005;41:321–331 [PubMed: 15768016]

39. Zhang L, Fu Z, Li X, Tang H, Luo J, Zhang D, Zhuang Y, Han Z, Yin M. Transforming growth factor beta-activated kinase 1 inhibitor suppresses the proliferation in triple-negative breast cancer through tgf-beta/tgfr pathway. Chemical biology & drug design. 2017;90:450–455 [PubMed: 28224764]
40. Watson CJF, Maguire ARR, Rouillard MM, Crozier RWE, Yousef M, Bruton KM, Fajardo VA, MacNeil AJ. Tak1 signaling activity links the mast cell cytokine response and degranulation in allergic inflammation. Journal of leukocyte biology. 2020
41. Delaney JR, Mlodzik M. Tgf-beta activated kinase-1: New insights into the diverse roles of tak1 in development and immunity. Cell cycle (Georgetown, Tex.). 2006;5:2852–2855
42. Ajibade AA, Wang HY, Wang RF. Cell type-specific function of tak1 in innate immune signaling. Trends in immunology. 2013;34:307–316 [PubMed: 23664135]
43. Li L, Chen Y, Li J, Yin H, Guo X, Doan J, Molkentin JD, Liu Q. Tak1 regulates myocardial response to pathological stress via nfat, nfkappab, and bnip3 pathways. Scientific reports. 2015;5:16626 [PubMed: 26564789]
44. Ji YX, Zhang P, Zhang XJ, Zhao YC, Deng KQ, Jiang X, Wang PX, Huang Z, Li H. The ubiquitin e3 ligase traf6 exacerbates pathological cardiac hypertrophy via tak1-dependent signalling. Nature communications. 2016;7:11267
45. Wu L, Mei L, Chong L, Huang Y, Li Y, Chu M, Yang X. Olmesartan ameliorates pressure overload-induced cardiac remodeling through inhibition of tak1/p38 signaling in mice. Life sciences. 2016;145:121–126 [PubMed: 26706286]
46. Chen L, Huang J, Ji YX, Mei F, Wang PX, Deng KQ, Jiang X, Ma G, Li H. Tripartite motif 8 contributes to pathological cardiac hypertrophy through enhancing transforming growth factor beta-activated kinase 1-dependent signaling pathways. Hypertension. 2017;69:249–258 [PubMed: 27956576]
47. Wu L, Cao Z, Ji L, Mei L, Jin Q, Zeng J, Lin J, Chu M, Li L, Yang X. Loss of tradd attenuates pressure overload-induced cardiac hypertrophy through regulating tak1/p38 mapk signalling in mice. Biochem Biophys Res Commun. 2017;483:810–815 [PubMed: 28013046]
48. Sakurai H Targeting of tak1 in inflammatory disorders and cancer. Trends in pharmacological sciences. 2012;33:522–530 [PubMed: 22795313]
49. Roh YS, Song J, Seki E. Tak1 regulates hepatic cell survival and carcinogenesis. Journal of gastroenterology. 2014;49:185–194 [PubMed: 24443058]
50. Santoro R, Carbone C, Piro G, Chiao PJ, Melisi D. Tak-ing aim at chemoresistance: The emerging role of map3k7 as a target for cancer therapy. Drug resistance updates : reviews and commentaries in antimicrobial and anticancer chemotherapy. 2017;33–35:36–42
51. Shi L, Chang Y, Yang Y, Zhang Y, Yu FS, Wu X. Activation of jnk signaling mediates connective tissue growth factor expression and scar formation in corneal wound healing. PloS one. 2012;7:e32128
52. Tsukada S, Westwick JK, Ikejima K, Sato N, Rippe RA. Smad and p38 mapk signaling pathways independently regulate alpha1(i) collagen gene expression in unstimulated and transforming growth factor-beta-stimulated hepatic stellate cells. J Biol Chem. 2005;280:10055–10064 [PubMed: 15647278]
53. Amento EP, Ehsani N, Palmer H, Libby P. Cytokines and growth factors positively and negatively regulate interstitial collagen gene expression in human vascular smooth muscle cells. Arteriosclerosis and thrombosis : a journal of vascular biology. 1991;11:1223–1230 [PubMed: 1911708]
54. Pera T, Sami R, Zaagsma J, Meurs H. Tak1 plays a major role in growth factor-induced phenotypic modulation of airway smooth muscle. American journal of physiology. Lung cellular and molecular physiology. 2011;301:L822–828 [PubMed: 21873447]
55. Naito H, Iba T, Wakabayashi T, Tai-Nagara I, Suehiro JI, Jia W, Eino D, Sakimoto S, Muramatsu F, Kidoya H, Sakurai H, Satoh T, Akira S, Kubota Y, Takakura N. Tak1 prevents endothelial apoptosis and maintains vascular integrity. Developmental cell. 2019;48:151–166 e157 [PubMed: 30639056]

56. Yang L, Joseph S, Sun T, Hoffmann J, Thevissen S, Offermanns S, Strilic B. Tak1 regulates endothelial cell necroptosis and tumor metastasis. Cell Death Differ. 2019;26:1987–1997 [PubMed: 30683914]

57. Lee ES, Boldo LS, Fernandez BO, Feelisch M, Harmsen MC. Suppression of tak1 pathway by shear stress counteracts the inflammatory endothelial cell phenotype induced by oxidative stress and tgf-beta1. Scientific reports. 2017;7:42487 [PubMed: 28209993]

58. Ohno M, Cooke JP, Dzau VJ, Gibbons GH. Fluid shear stress induces endothelial transforming growth factor beta-1 transcription and production. Modulation by potassium channel blockade. The Journal of clinical investigation. 1995;95:1363–1369 [PubMed: 7883983]

59. Cucina A, Sterpetti AV, Borrelli V, Pagliei S, Cavallaro A, D'Angelo LS. Shear stress induces transforming growth factor-beta 1 release by arterial endothelial cells. Surgery. 1998;123:212–217 [PubMed: 9481408]

60. Negishi M, Lu D, Zhang YQ, Sawada Y, Sasaki T, Kayo T, Ando J, Izumi T, Kurabayashi M, Kojima I, Masuda H, Takeuchi T. Upregulatory expression of furin and transforming growth factor-beta by fluid shear stress in vascular endothelial cells. Arterioscler Thromb Vasc Biol. 2001;21:785–790 [PubMed: 11348875]

Highlights

- TAK1 is upregulated in human and mouse mature arteriovenous fistulae (AVF).
- TAK1 regulates AVF maturation *in vivo*, and increasing TAK1 activity increases both AVF wall thickening and diameter.
- Mouse endothelial cells exposed to arterial magnitudes of laminar shear stress show increased TAK1 signaling.

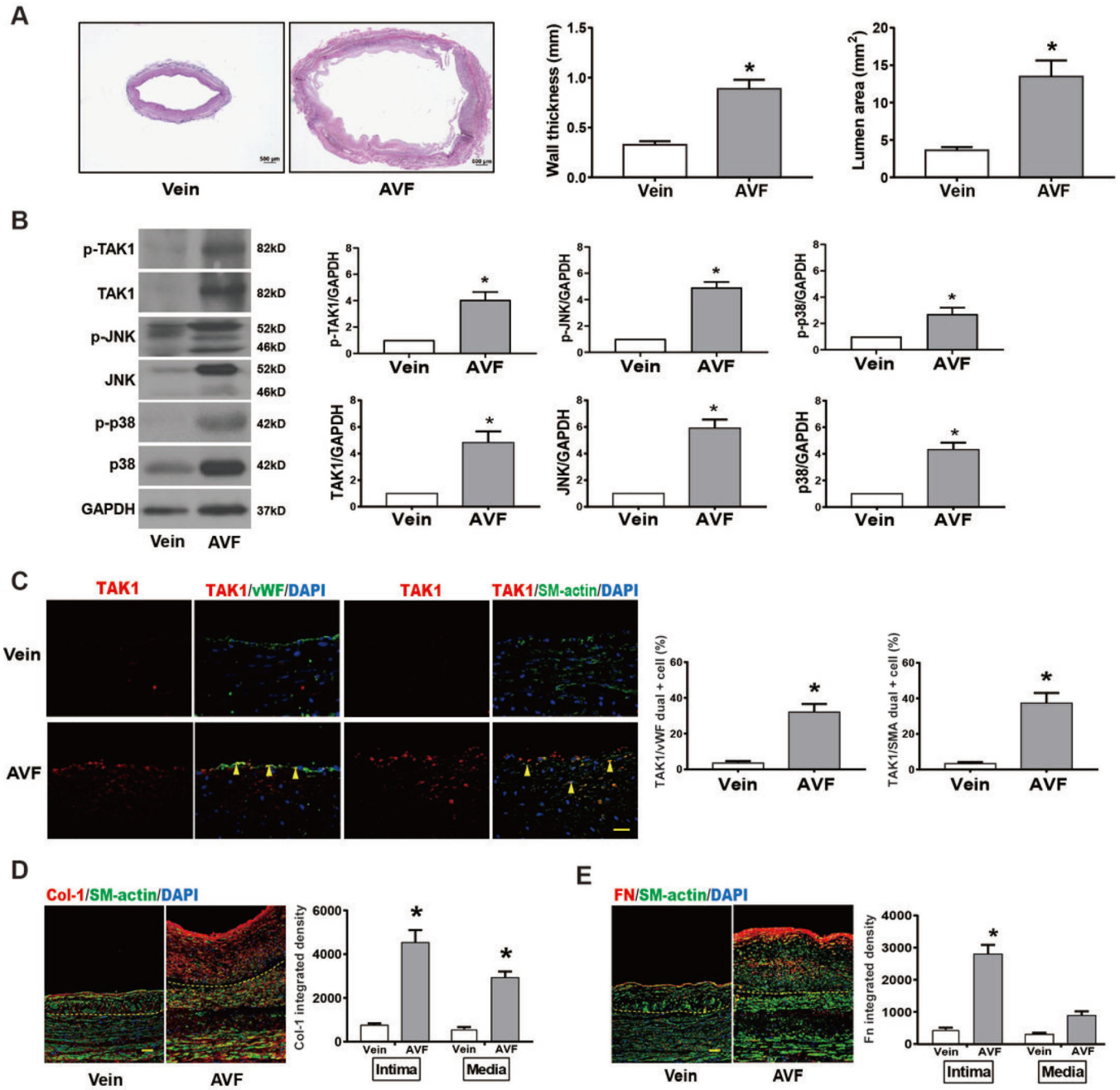

Fig 1. TAK1 is upregulated in human mature AVF.

(A) Representative human control vein (**left**) and human matured AVF (**right**) by Elastin Von Gieson (EVG) staining (n=3 for each group), scale bar, 500 μm. Adjacent bar graphs showing wall thickness and vessel dilation by lumen area in the human control vein and matured AVFs (p=0.0002, wall thickness; p=0.0043, lumen area). **(B)** Representative Western blots and adjacent graphical quantification showing increased p-TAK1 (p=0.0076), TAK1 (p=0.065), p-JNK (p=0.0008), JNK (p=0.0017), p-p38 (p=0.0134), p38 (p=0.0032) (n=3 each). **(C)** Representative immunofluorescence images showing the venous limbs of human mature AVF and control vein, scale bar 25 μm. Adjacent bar graphs show increased

expression in endothelial cells (n=3 each; p=0.0091), and smooth muscle cells (n=3; p=0.0015). **(D)** Representative images showing expression of collagen I in human mature AVF, compared to control veins without AVF (dash lines showing internal elastic lamina); scale bar, 100 μm. Adjacent bar graphs show quantification of collagen I in the intima or media in each group (n=3 each; p<0.0001 in intima and p=0.0015 in media). **(E)** Representative images showing expression of fibronectin in human mature AVF, compared to control veins without AVF; scale bar, 100 μm. Adjacent bar graphs show quantification of fibronectin in the intima or media in each group (n=3 each; p<0.0001 in the intima). Statistical tests used: Student's *t* test.

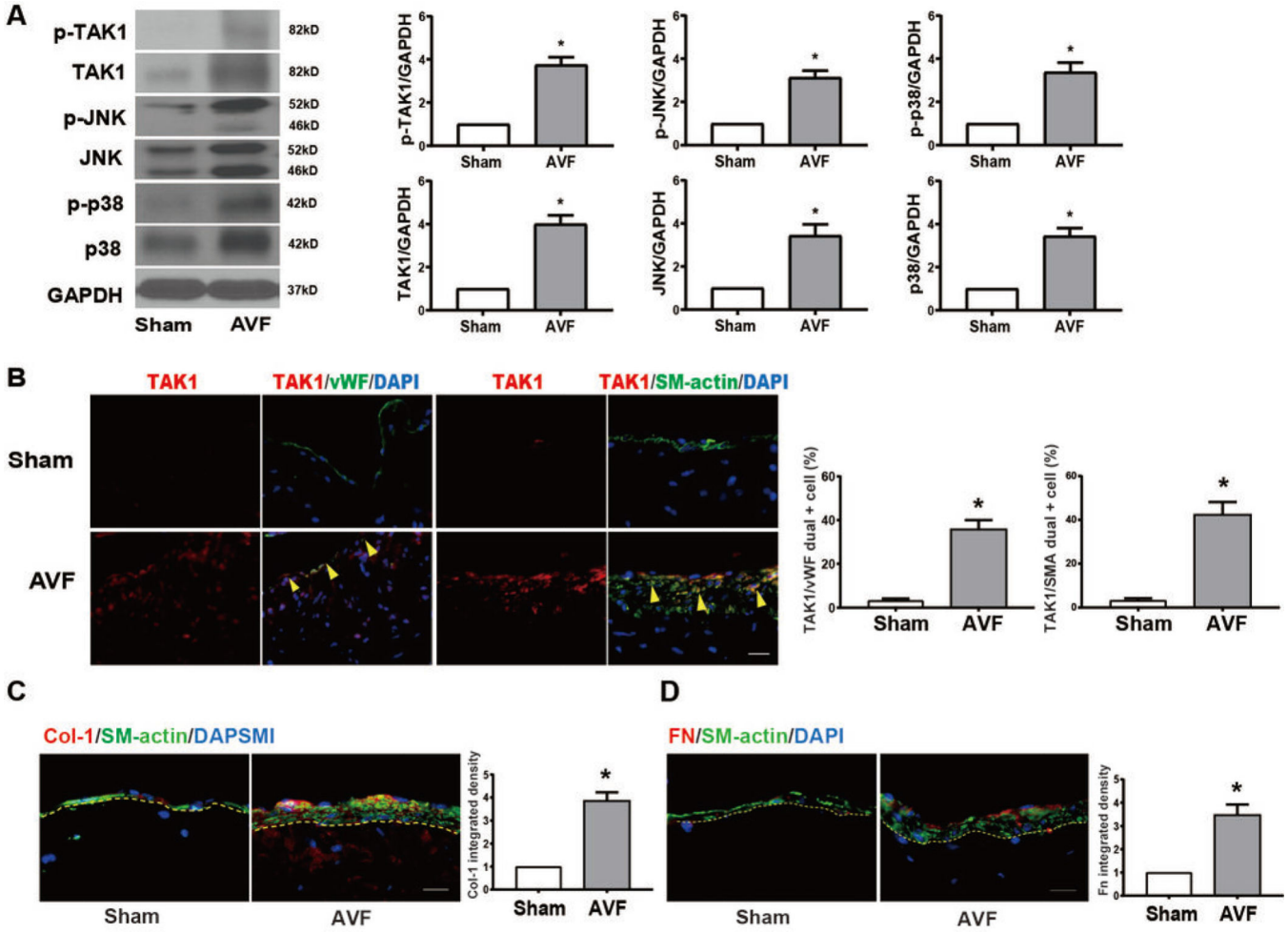

Fig. 2. TAK1 is upregulated during AVF maturation in a mouse AVF model.

(A) Representative Western blot images and quantitative data showing increased protein expression of p-TAK1 (p=0.015), TAK1 (p=0.0012), p-JNK (p=0.0027), JNK (p=0.0051), p-p38 (p=0.0056), p38 (p=0.0099), in AVF, normalized to GAPDH (n=3). **(B)** Representative images showing TAK1 expression in the IVC of sham-operated mice or AVF (n=4); scale bar, 100 μm. Adjacent bar graphs show expression of TAK1 in the endothelial cells (n=4; p=0.0019, *t* test) or SMC (n=4; p=0.0026). **(C)** Representative images and summary bar graph showing expression of collagen I in AVF (day 21), compared to IVC (n=3; p=0.0016), scale bar, 100 μm. **(D)** Representative images and summary bar graph showing expression of fibronectin in AVF and IVC (n=3; p=0.0056), scale bar, 100 μm. Statistical tests used: Student's *t* test.

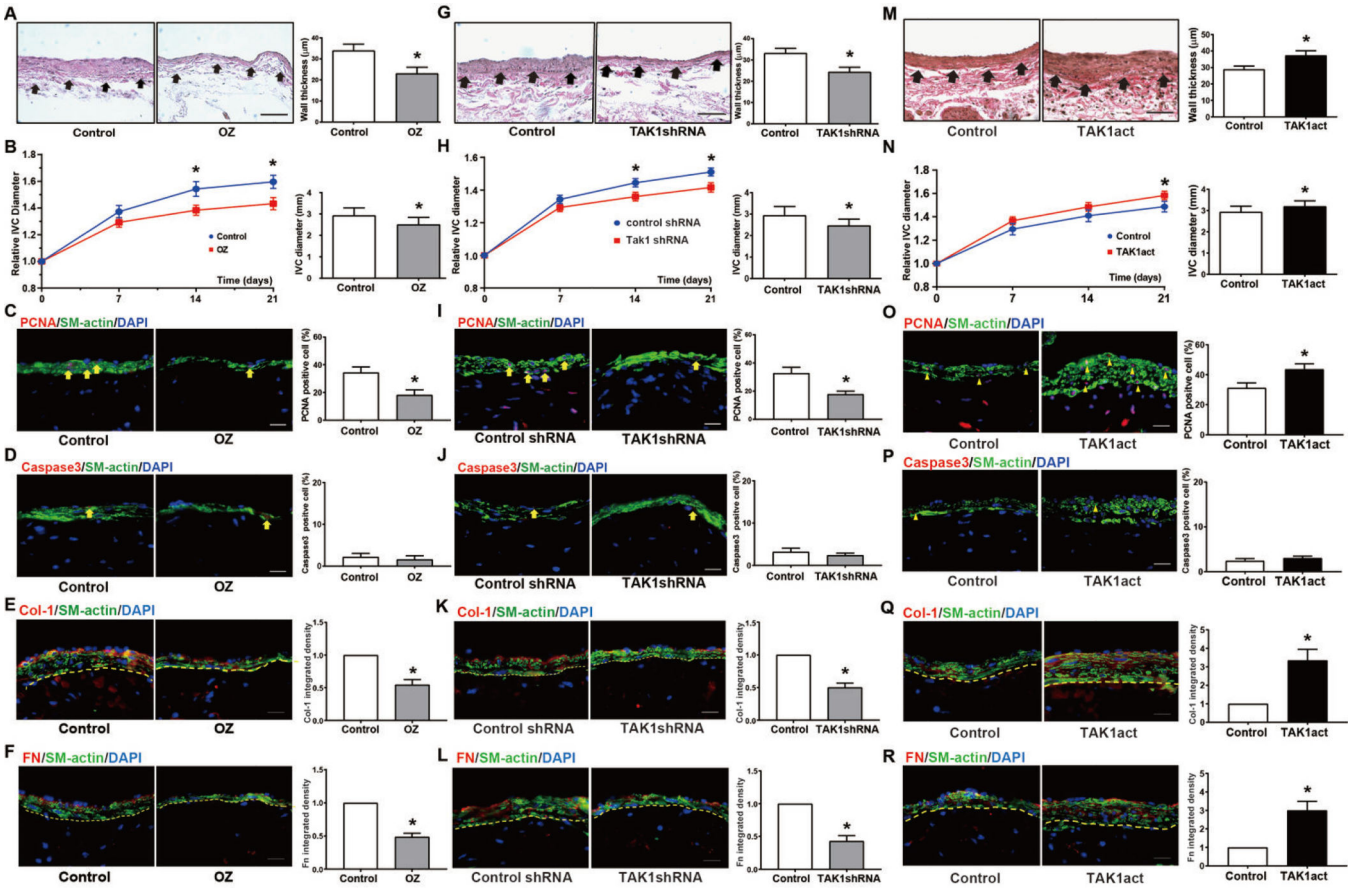

Fig.3. manipulation regulates AVF wall thickening and dilation during AVF maturation.

(A) EVG stains demonstrating AVF thickening in vehicle treated or 5Z-7-oxozeaenol (OZ) treated mice at post-op day 21 after AVF. Yellow arrowheads show the medial-adventitial boundary. Adjacent bar graph shows group wall thickness (n=4; p=0.0326). **(B)** Fold-change in infrarenal IVC diameter after AVF in DMSO-injected or OZ-injected mice (n=20; p=0.02 at day 14, p=0.02 at day 21). Adjacent bar graph shows IVC diameter at day 21, (n=10; p=0.01). **(C)** PCNA immunofluorescence images in AVF of DMSO or OZ-treated IVC at day 21. Summary bar graph shows percentage of PCNA positive cells (n=10, p<0.01). **(D)** Caspase-3 immunofluorescence images in AVF of DMSO or OZ-treated IVC at day 21. Summary bar graph shows percentage of caspase-3 positive cells (n=10, p=0.31). **(E)** Col1 immunofluorescence images in AVF of DMSO or OZ-treated IVC at day 21. Summary bar graph shows integrated density of col1 within vascular wall (within dashed line) (n=6, p<0.01). **(F)** Fibronectin immunofluorescence images in AVF of DMSO or OZ-treated IVC at day 21. Summary bar graph shows integrated density of Fn within vascular wall (within dashed line) (n=10, p<0.01). **(G-L)** Similar experiments with periadventitially-delivered control (scrambled) shRNA or TAK1-specific shRNA. Compared to control, TAK1 shRNA treated animals at day 21 have **(G)** decreased wall thickness (n=10, p=0.02), **(H)** decreased luminal diameter (n=16; for line graphs: p=0.03 at day 14; p=0.01 at day 21; for bar chart: p=0.0195), **(I)** reduced PCNA (n=10, p=0.01), **(J)** unchanged caspase-3 (n=10, p=0.45), **(K)** decreased col1 (n=10, p<0.01), and **(L)** decreased fibronectin (n=10, p<0.01). **(M-R)** Similar

experiments with periadventitially-delivered control lentivirus or lentivirus carrying TAK1 activation particles (TAK1act). Compared to control, TAK1act AVF at day 21 have **(M)** increased wall thickness (n=12, p=0.04), **(N)** increased luminal diameter (n=24; for line graphs: p=0.23 at day 14; p=0.02 at day 21; for bar chart: p=0.04), **(O)** increased PCNA (n=10, p=0.04), **(P)** unchanged caspase-3 (n=10, p=0.4), **(Q)** increased col1 (n=10, p<0.01), and **(R)** increased fibronectin (n=10, p<0.01). Scale bars are 100μm. Data are presented as mean ± SEM. Statistical tests: Student's t test for bar graphs; Repeated measures 2-way ANOVA with Sidak's post-hoc test for line graphs.

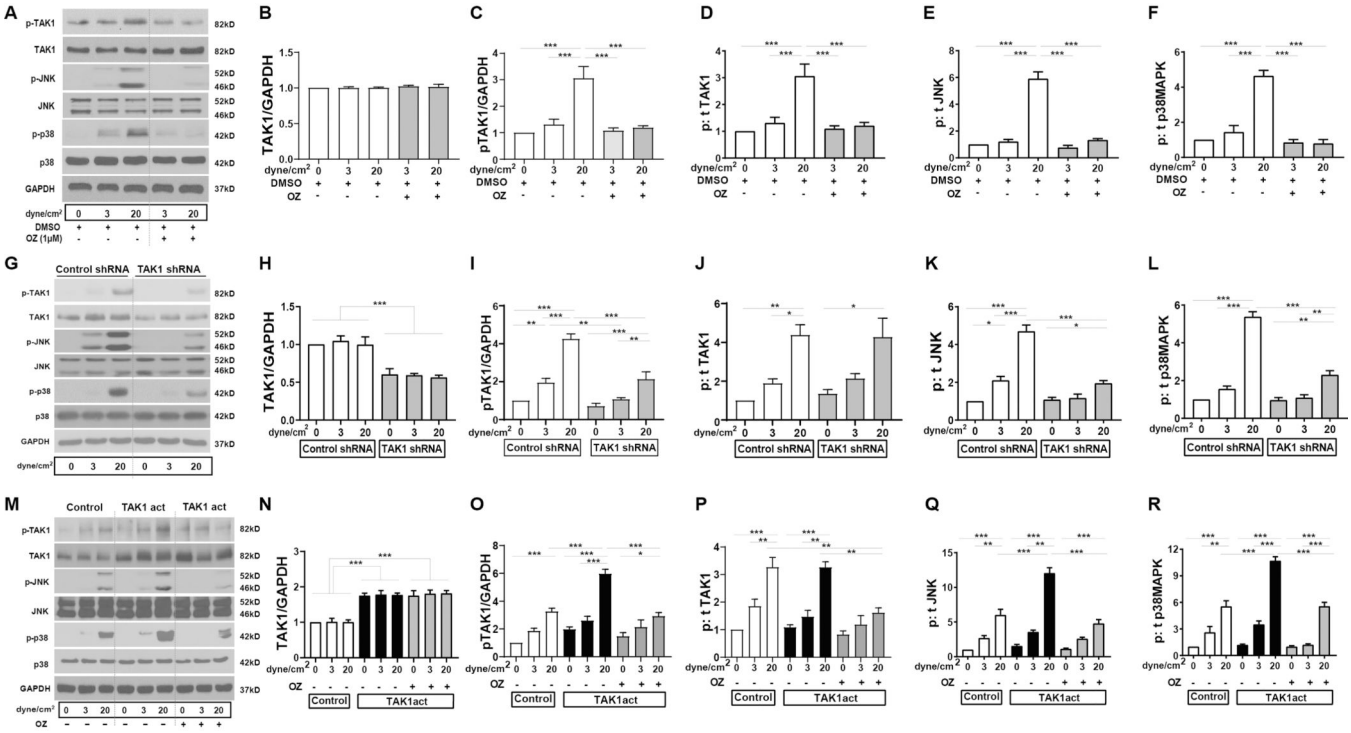

Figure 4. Increased shear stress mediates TAK1 phosphorylation in EC *in vitro*.

(A) Representative Western blots show expression of p-TAK1, TAK1, p-JNK, JNK, p-p38 and p38, and GAPDH in mouse lung EC under 0 (resting), 3 dyne/cm^2 (venous) or 20 dyne/cm^2 (arterial) laminar shear stress, with or without OZ pretreatment compared to DMSO. **(B-F)** Summary densitometry from n=3 independent experiments. **(G-L)** Similar experiments with EC treated with control (scrambled) shRNA or TAK1-specific shRNA with corresponding summary data (n=3). **(M-R)** Similar experiments with EC treated with control or TAK1 activation particle (TAK1act) carrying lentivirus with corresponding summary data (n=3). Data are presented as mean ± SEM. Comparisons were made using the two-way ANOVA with Tukey's post hoc tests. *p<0.05, **p<0.01, ***p<0.001.